The time course and chromosomal localization of recombination-related proteins at meiosis in the mouse are compatible with models that can resolve the early DNA-DNA interactions without reciprocal recombination

Peter B. Moens[1,*], Nadine K. Kolas[1], Madalena Tarsounas[2], Edyta Marcon[1], Paula E. Cohen[3] and Barbara Spyropoulos[1]

[1]Department of Biology, York University, Toronto, ON, M3J 1P3, Canada
[2]Imperial Cancer Research Fund, South Hall Laboratories, South Mimms, Hertfordshire, England EN6 3LD
[3]Dept of Molecular Genetics, Albert Einstein College of Medicine, New York 10461 USA
*Author for correspondence (e-mail: moens@yorku.ca)

Accepted 11 December 2001
Journal of Cell Science 115, 1611-1622 (2002) © The Company of Biologists Ltd

Summary

During mouse meiosis, the early prophase RAD51/DMC1 recombination protein sites, which are associated with the chromosome cores and which serve as markers for ongoing DNA-DNA interactions, are in ten-fold excess of the eventual reciprocal recombinant events. Most, if not all, of these early interactions are eliminated as prophase progresses. The manner in which these sites are eliminated is the focus of this investigation. We report that these sites acquire replication protein A, RPA and the *Escherichia coli* MUTS homologue, MSH4p, and somewhat later the Bloom helicase, BLM, while simultaneously losing the RAD51/DMC1 component. Eventually the RPA component is also lost and BLM sites remain. At that time, the MUTL homologue, MLH1p, which is essential for reciprocal recombination in the mouse, appears in numbers and locations that correspond to the distribution of reciprocal recombination events. However, the MLH1 foci do not appear to coincide with the remaining BLM sites. The MLH1p is specifically localized to electron-microscope-defined recombination nodules. We consider the possibility that the homology-search RAD51/DMC1 complexes are involved in homologous chromosome synapsis but that most of these early DNA-DNA interactions are later resolved by the anti-recombination RPA/MSH4/BLM-topoisomerase complex, thereby preventing the formation of superfluous reciprocal recombinant events.

Key words: Meiosis, Recombination proteins, Immunocytology, synaptonemal complexes, BLM, RPA, MLH1, Mouse, Recombination nodules

Introduction

Although the number of reciprocal recombination events at meiosis is similar for organisms with widely different genome sizes such as the mouse and lily (which have between 20 and 50 events), the number of DNA-DNA interactions that are recognized by RAD51/DMC1p immunocytology at prophase of meiosis is much higher (250 for the mouse and more than 2000 for lily) (Anderson et al., 2001). It follows that most or all of these early interactions do not necessarily function in the formation of reciprocal events. Conceivably, the numbers relate to genome size, 3.3 pg for the mouse and 141 pg for lily. However, the genome sizes differ by a factor of 43, whereas the number of RAD51/DMC1 foci in the mouse differs only by a factor of 10 from the lily. A better correlate appears to be the length of paired prophase chromosomes, as measured by the total length per nucleus of the synaptonemal complexes, SCs, which are the axes of the bivalents (about 200 μm for the mouse and about 3000 μm for lily). The tentative conclusion is that these foci, which are associated with the chromosome cores and SCs, function in SC formation (Anderson et al., 2001). Synaptic failure in the absence of RAD51/DMC1 foci in SPO11$^{-/-}$ mice also suggests a role for early nodules in synapsis (Baudat et al., 2000; Romanienko and Camerini-Otero, 2000).

Molecular models for the resolution of DNA-DNA interactions without reciprocal recombination have been discussed by Gilbertson and Stahl (Gilbertson and Stahl, 1996) and involve helicase-topoisomerase activity to resolve joint molecules. The acquisition of replication protein A, RPA and Bloom mutated protein, BLM, at the RAD51/DMC1 sites might be the physical manifestation of the models – RPA may stimulate BLM-RecQ helicase activity (Brosh et al., 2000) in concert with topoisomerase IIIa (Johnson et al., 2000) to resolve the early DNA-DNA interactions at the RAD51/DMC1 sites.

The development of reciprocal genetic exchange events at meiosis in many fungi, plants and animals can be monitored at several levels: (1) at the chromosomal level by chiasmata, which are the sites of reciprocal recombination (Jones, 1987); (2) by the recombination nodules, RNs, which correlate with

genetic and cytological patterns of recombination (Carpenter, 1975; Carpenter, 1979; Albini and Jones, 1988); and (3) by the MLH1p sites, which are associated with crossover sites (Anderson et al., 1999)

Nodules are SC-associated, electron-microscope-defined structures that have been reported in the meiocytes of protists, fungi, plants and animals. In early meiotic prophase, 'nodules' refer to the several hundreds of small dense bodies about 100 nm in diameter that are associated with chromosome cores and SCs and contain the RAD51/DMC1 proteins in lily (Anderson et al., 1997), mouse and human (Haaf et al., 1995; Moens et al., 1997; Barlow et al., 1997). Since the correlation of these structures with reciprocal recombination is tenuous, they are usually referred to as 'early nodules', EN. The late RNs, as originally defined by Carpenter (Carpenter, 1975) in *Drosophila melanogaster* oocyte SCs, correspond in number and location to reciprocal recombinant events in normal and mutant *D. melanogaster*. In the rat, 'late RNs' are well defined electron-dense bodies of variable shape and size, 100 to 200 nm, located on the mature SC at pachytene stage VII of the spermatogenic pathway but not in earlier pachytene stages I to V (Clermont, 1972; Moens, 1978). Cross-sectioned SCs and whole-mount, shadow-cast EM preparations show that RNs are located on the surface of the SC either along the central element or obliquely across the SC (Fig.7). The reported number of late RNs (19 to 22 per nucleus) in complete EM-reconstructed rat-pachytene nuclei, their non-random distribution and their association with MLH1 (Mut L homolog) protein in rat and mouse (this report), agree with their proposed function in reciprocal recombination by Carpenter (Carpenter, 1975; Carpenter, 1979). A number of publications have assigned various proteins to RNs but the assignments have not previously been verified by EM demonstration of these proteins on the RNs.

We report the events in individual mouse and rat spermatocyte nuclei from early to late meiotic prophase in terms of chromosome core behavior and associated protein complexes. The immunofluorescence observations are refined and detailed by immunoelectron microscopy of the recombination-related proteins and by EM visualization of RNs. These observations are interpreted in the context of the chromosome synapsis and reciprocal recombination and discussed in relation to reports by others on these events.

Materials and Methods

Cell preparation

The nuclear contents of whole-mount spermatocyte were displayed by surface spreading of a testicular cell suspension on a hypotonic liquid surface (Counce and Meyer, 1973; Dresser and Moses, 1980). The intact nuclei became attached to a plastic-coated glass slides and were fixed briefly with a 2% paraformaldehyde with 0.03% SDS to permeabilize the nuclear envelope. After washing and drying in the presence of the wetting agent, Kodak Photo-Flo 200, the cells were blocked with goat serum and incubated overnight with primary antibodies at room temperature (Dobson et al., 1994). For EM, the cells are treated for 10 minutes with 1 μg DNase per ml MEM to make the SCs and SC-associated proteins more accessible to immunogold grains (Moens et al., 1987). After washes, the cells were incubated for 1 hour at 37°C with fluorochrome or colloidal gold-conjugated secondary antibodies. After washes, the cells were mounted in ProLong Antifade (Molecular Probes) for fluorescence microscopy or the plastic is floated off and transferred to EM grids (Dobson et al., 1994). The EM grids were treated with alcoholic phosphotungstic acid (PTA) or a shadow cast at an angle of 7° with platinum-gold (Moens et al., 1987). For rapid advancement of early prophase cells into the diplotene stage, cells were treated for 2 hours with the phosphatase inhibitor okadaic acid (Tarsounas et al., 1999b).

Antibodies

Polyclonal rabbit antibodies against whole hamster SCs and polyclonal mouse antibodies against the fusion proteins of the hamster 30 kDa chromosome core protein, COR1p, and the 125 kDa synaptic protein SYN1p have been characterized previously (Dobson et al., 1994; Tarsounas et al., 1997; Tarsounas et al., 1999a) and have been used extensively by others (Plug et al., 1997; Plug et al., 1998; Pittman et al., 1998). The equivalent rat 30/33 and 125 kDa SC proteins are named SCP3p and SCP1p (Heyting et al., 1988). From J. Ingles, University of Toronto, we received the polyclonal rabbit anti-RPA antibody (Henricksen et al., 1994; He et al., 1995), which has also been used for similar experiments on RPA at meiosis (Plug et al., 1997; Plug et al., 1998). From J. Masson (ICRF, UK), we received the recombinant HsRPA with the 14, 32 and 70 kDa subunits identified with western blotting. Our mouse, 23LM, produced a polyclonal anti-RPA serum against this recombinant HsRPA with good fluorescent and EM immunocytology. Centromeres were labeled with a CREST serum as reported earlier (Dobson at al., 1994). The rabbit anti-BLM antibody was raised against the purified fusion protein of the last 380 amino acids of BLMp. The antiserum recognized the appropriate 180 kDa protein in western blots of HeLa whole-cell extracts, and no protein was detected in the BS cell line that lacked the BLMp C-terminal portion (Moens et al., 2000). Mouse full-length, (His)6-tagged DMC1 and RAD51 proteins were overexpressed in *Escherichia coli*. The Ni-NTA-purified proteins were injected into mice and rabbits that had negative pre-immune serum. Both types of sera cross-react with RAD51p and DMC1p, but after immune depletion, they were rendered specific for one or the other antigen. Because it was shown with fluorescence and EM cytology of the purified antibodies that the two antigens colocalize on mouse and rat SC-associated early nodules (Tarsounas et al., 1999a), we used,for this study, the anti-DMC1 serum from our rabbit 'Patch' or mouse '17RB' to detect the mixed RAD51/DMC1 antigen in core/SC-associated early nodules. These anti-RAD51/DMC1p antibodies differ from those used in a number of earlier reports in that they do not contain anti-SC antibodies, which are common contaminants of rabbit serum (Ashley et al., 1995; Kovalenko et al., 1996; Moens et al., 1997). The monoclonal anti-MLH1p antibody was obtained from BD Pharmingen and has been characterized by Edelmann et al. (Edelmann et al., 1996) and Anderson et al. (Anderson et al., 1999). The polyclonal anti-hMSH4 was generated in rabbit and has been characterized by Santucci-Darmanin et al. (Santucci-Darmanin et al., 2000). Antibodies against rat testis-specific histone H1t were generated in a rabbit with *E. coli*-expressed H1t protein (Kremer and Kistler, 1991; Moens, 1995).

Imaging

Fluorescence from FITC- or rhodmamine-tagged secondary antibodies and DAPI-stained chromatin was recorded by CCD camera or single or multiple exposures of black and white or colour-positive film, ASA 400. Slides were scanned at 1,000 dpi and recorded in TIFF format, and final images were arranged with Adobe PhotoDeluxe software. Images were reproduced with an Epson 700 or 870 colour printer. To determine the colocation of RPA with BLM foci, the images were recorded on black and white film and one positive and one negative image were superimposed. Electron micrographs of cores/SCs and immunogold were recorded at various magnifications, 1 k to 10 k, and photographically enlarged. The contrast of SCs and

nodules in EM preparations was enhanced by staining for 30 minutes in 4% alcoholic PTA followed by a rinse with 95% ethanol. Shadow-casting of SCs was achieved by gold-palladium evaporation at a low angle of 7° on stationary or rotary moving grids (Moens et al., 1987).

Results

Staging of meiotic prophase nuclei.

For the purpose of this study, it is essential that the successive developmental prophase stages of the mouse male meiotic prophase nuclei are accurately defined. The traditional criteria of SC formation, X-Y pairing and chromosome separation are not always sufficient by themselves. A greater accuracy can be obtained by a combination of these structural characteristics and monitoring the presence or absence of proteins that function at different stages of meiotic prophase.

(1) Early prophase: the leptotene stage. With CREST serum, there are 40 immunofluorescent centromeres, which are frequently arranged in a few groups. The anti-COR1/SCP3 antibodies recognize short chromosomal core segments. There is no staining of synapsed core segments with anti SYN1/SCP1 antibodies. Anti-RAD51 or DMC1 antibodies visualize up to 300 core/SC-associated immunofluorescent foci. Other recombination-related proteins, BLM, RPA, MSH4 and MLH1 are not present or rare. Antibodies against testis-specific histone 1, H1t, do not cause fluorescence of the chromatin (Moens, 1995).

(2) Early prophase: the synaptic or zygotene stage. A variable number of centromeres are in pairs. The chromosome cores are single or partially synapsed, and the synapsed segments are recognized by the anti-SYN1/SCP1 antibodies. The increasing lengths of the synapsed regions are a measure of progression through the synaptic stage. The cores of the X and Y chromosomes are not distinct from the autosomes. The numbers of RAD51/DMC1 are in decline, from about 200 to 100 or less. The core and SC-associated RPA and BLM foci become numerous, up to about 200 per nucleus, and these, too, decline at the late synaptic stage. MSH4 foci appear during zygotene, but MLH1 foci are not normally present at this time. The partially synapsed bivalents occasionally cause the nucleus to resemble the late prophase diplotene stage. However, at diplotene the recombination-associated proteins are not normally present, and the paired centromeres mostly stay together (unlike the zygotene stage where they often are the last to pair). Also, the chromatin of diplotene but not zygotene nuclei is H1t positive.

(3) The fully synapsed pachytene stage. Except for an occasional bivalent that is lagging in synapsis, all the autosomes are fully synapsed so that the immune staining patterns of autosomes with anti-SYN1/SCP1 and COR1/SCP3 are the same. The X and Y chromosomes are partially paired, but there is not a distinct sex body or sex vesicle associated with the sex chromosomes at the early pachytene stage. At the later pachytene stages, the X and Y are embedded in a sex vesicle. There is a spherical 400 nm double dense body, DDB, associated with the X chromosome, which is visible in EM images. The number of autosomal RAD51/DMC1 foci declines to zero, but the foci of the unpaired X chromosome persist into mid or late pachytene. There are 100 or fewer RPA, MSH4 and BLM foci. The MLH1 foci appear for the first time and are present in small numbers, up to an average of 26 as reported by Anderson et al. (Anderson et al., 1999) and in somewhat higher numbers as observed by us. At mid pachytene, the chromatin becomes positive for testis-specific histone 1, H1t. The DDB is no longer associated with the X chromosome.

(4) Late prophase: the repulsion stage. The main chromosomal characteristic of this stage is the partial separation of chromosome cores. The remaining paired segments have immune staining with an anti-SYN1/SCP1 antibody, and there are progressively shorter and fewer of these segments. There are no recombination protein foci at the SCs or the cores under normal circumstances. Many of the centromeres remain in pairs. COR1/SCP1 protein is present until diplotene progresses to metaphase I, at which time the cores become fragmented but the protein remains associated with sister centromeres until anaphase II. The chromatin is positive for antibodies to testis-specific histone H1t. The sex vesicle contains much elongated, sinuous X and Y chromosome cores and is positive for a variety of antibodies (Turner et al., 2000).

Time course of RAD51/DMC1p versus RPA foci on meiotic chromosome cores/SCs

The RAD51/DMC1 foci of the meiotic prophase chromosomes are the sites of single-strand DNA tails that are active in homology search and strand exchange (Bishop, 1994; Schwacha and Kleckner, 1997). The presence of RPA protein in relation to RAD51/DMC1 foci at successive developmental stages of mouse spermatocyte nuclei at meiotic prophase is illustrated in Fig. 1. The number and intensity of immunofluorescent RPA foci increases from the time the chromosome cores first form and synapse at the zygotene stage of meiosis until late in the fully synapsed state at pachytene. The relative proportions of RAD51/DMC1 and RPA foci in individual nuclei can be demonstrated with simultaneous visualization of the two types of foci. In Fig. 1A and B, the early prophase nucleus to the left of the white line is in the leptotene/zygotene stage, judging by the mostly unpaired centromeres (enhanced red). This nucleus has an abundance of RAD51/DMC1 foci (about 200) (Fig. 1A), but a maximum of only 90 weak RPA foci (Fig. 1B). At a later stage, judging by the paired centromeres and the aligned foci, there are fewer DMC1 foci (approximately 90) in the nucleus on the right side of Fig. 1A, while the number of RPA foci has increased to 180 in that same nucleus (Fig. 1B).

The comparisons of Fig. 1A with B are reliable since the respective nuclei are in the same preparation and therefore received the same treatments. The shift from RAD51/DMC1 foci to RPA foci is a general characteristic of developmental progression of the prophase nucleus. The replacement is not necessarily synchronous for individual chromosomes. In Fig. 1D, SC#1 has acquired a full complement of RPA foci, and the RAD51/DMC1 component is almost completely eliminated judging by the absence of aligned foci in SC#1 of Fig. 1C. The same is true for SC#2. On the other hand SC#3 has aligned RAD51/DMC1 foci but few and indistinct RPA foci.

RPA replaces RAD51/DMC1p

With the abundance of the two types of foci along the SCs, it is likely that by chance alone the two types will be close together,

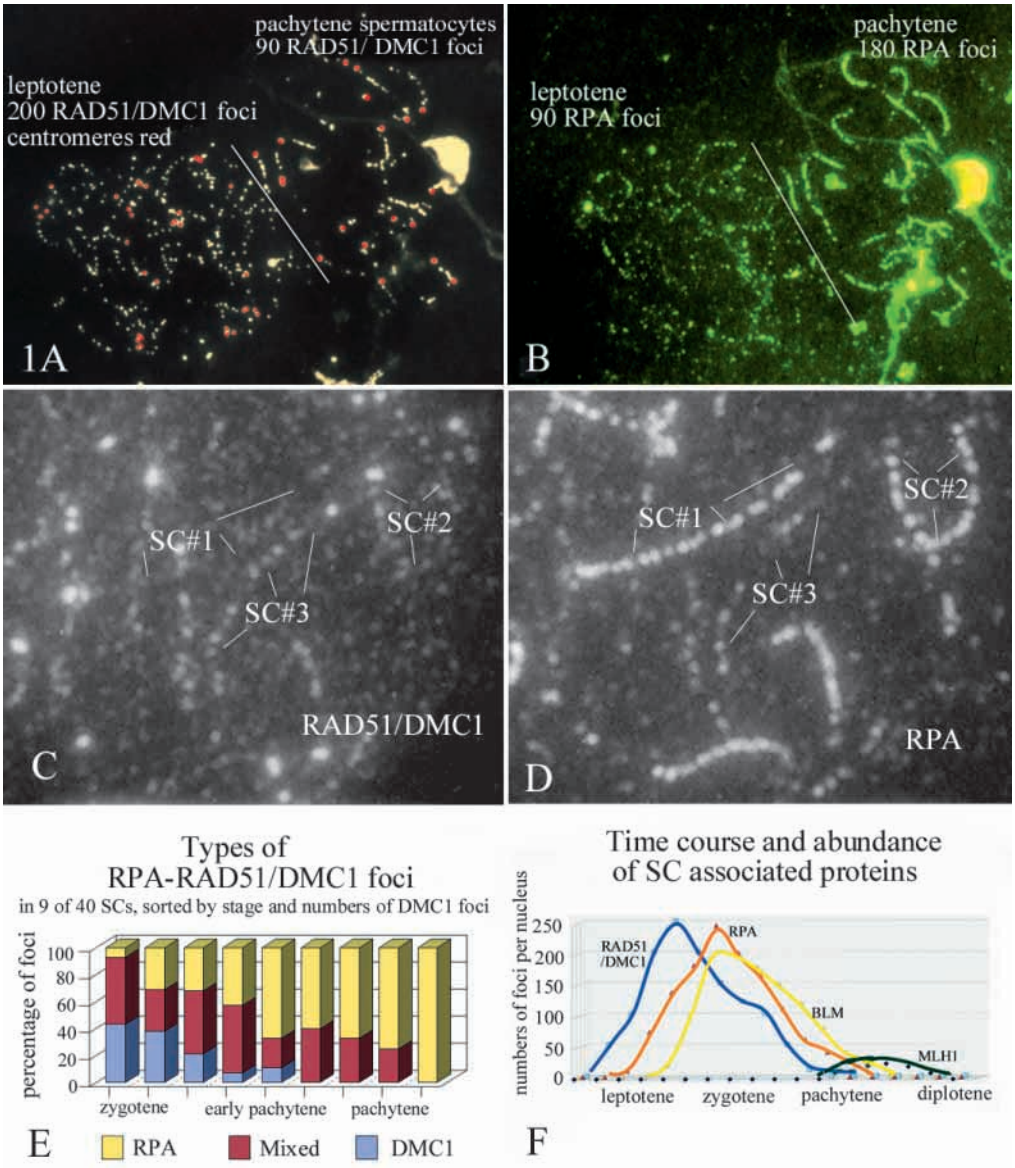

Fig. 1. Time course and interactions of SC-associated RAD51/DMC1, RPA and BLM protein in mouse spermatocytes. (A,B) RAD51/DMC1 foci initiate prior to detection of RPA. To the left of the white line is a spermatocyte early zygotene nucleus with mostly unpaired centromeres (red), which has about 200 RAD51/DMC1 foci (yellow). A nucleus in a later stage of meiotic prophase to the right of the line has fewer, about 90, foci. The same two nuclei stained for RPA in Fig. 1B show that the early prophase nucleus on the left has few and indistinct RPA foci, whereas the pachytene nucleus to the right of the line has an abundance of RPA foci. (C,D) The shift from RAD51/DMC1 to RPA foci is a developmental progression for the nucleus as a whole, but details seem to be regulated at the level of the individual bivalent. SC#1 and 2 have acquired a full complement of RPA foci (1D) and have lost most RAD51/DMC1 foci (1C), whereas SC#3 still has RAD51/DMC1 foci but few and indistinct RPA foci. (E) The replacement of RAD51/DMC1 by RPA is demonstrated from the relative amounts of the two proteins in individual foci based on electron microscopy of two types of immunogold grains as in Fig. 2. The data from nine of 40 SCs are presented in a bar graph; the top portion is the percentage of foci with only RPA antigen, the middle portion represents the foci with both antigens, and the lower part is the percentage of pure RAD51/DMC1 foci. Each bar represents one SC, and the SCs were sorted according to the prophase stage of the nucleus and by the previously documented decline in RAD51/DMC1 foci from zygotene to pachytene (details in Materials and Methods). The composition of the protein complexes change at successively later stages of meiotic prophase. (F) The line graph shows the number of fluorescent foci at progressively later stages of prophase. RAD51/DMC1 peaks at leptotene. Somewhat later, RPA reaches its maximum and later still, BLM does. These three antigens frequently are present together in individual foci. MLH1 appears at late prophase and is present in low numbers. Each data point is one nucleus, and the staging of the nuclei is described in the Materials and Methods.

and it is difficult at the level of immunofluorescence resolution to decide how much actual colocalization exists. At the high resolution of the electron micrographs in Fig. 2, it is possible to distinguish between pure RAD51/DMC1 foci (groups of 10 nm immunogold grains), pure RPA foci (5 nm gold grains) and mixed foci (colocation of 5 and 10 nm gold grains). The immunogold foci of 40 SCs were classified accordingly, and the percentages of the three types at progressively later prophase stages are shown for nine of the 40 SCs in the bar graph of Fig. 1E. It is evident from the brown middle segment of the first bar that most of the RPA protein initially colocalizes with the RAD51/DMC1 foci. The remainder of the bars suggest that the RPA gradually replaces the RAD51/DMC1 component of the foci to the point where there is no RAD51/DMC1 protein (last bar in Fig. 1E). While it is possible that the mixed foci arise de novo, the gradient of the percentages of the two types of proteins would favour a dynamic replacement process. The total numbers of immunofluorescent foci per nucleus for successive developmental stages is demonstrated in Fig. 1F. Many of these would be in mixed foci as shown in Fig. 1E, Fig. 2C and Fig. 4.

At high resolution, the abundance of RAD51/DMC1 foci and the paucity of RPA protein at the onset of chromosome synapsis is illustrated in the electron micrograph of a set of partially synapsed cores in Fig. 2A. There are six or seven groups of 10 nm RAD51/DMC1-associated immunogold grains but only one group and a few sporadic 5 nm, RPA-

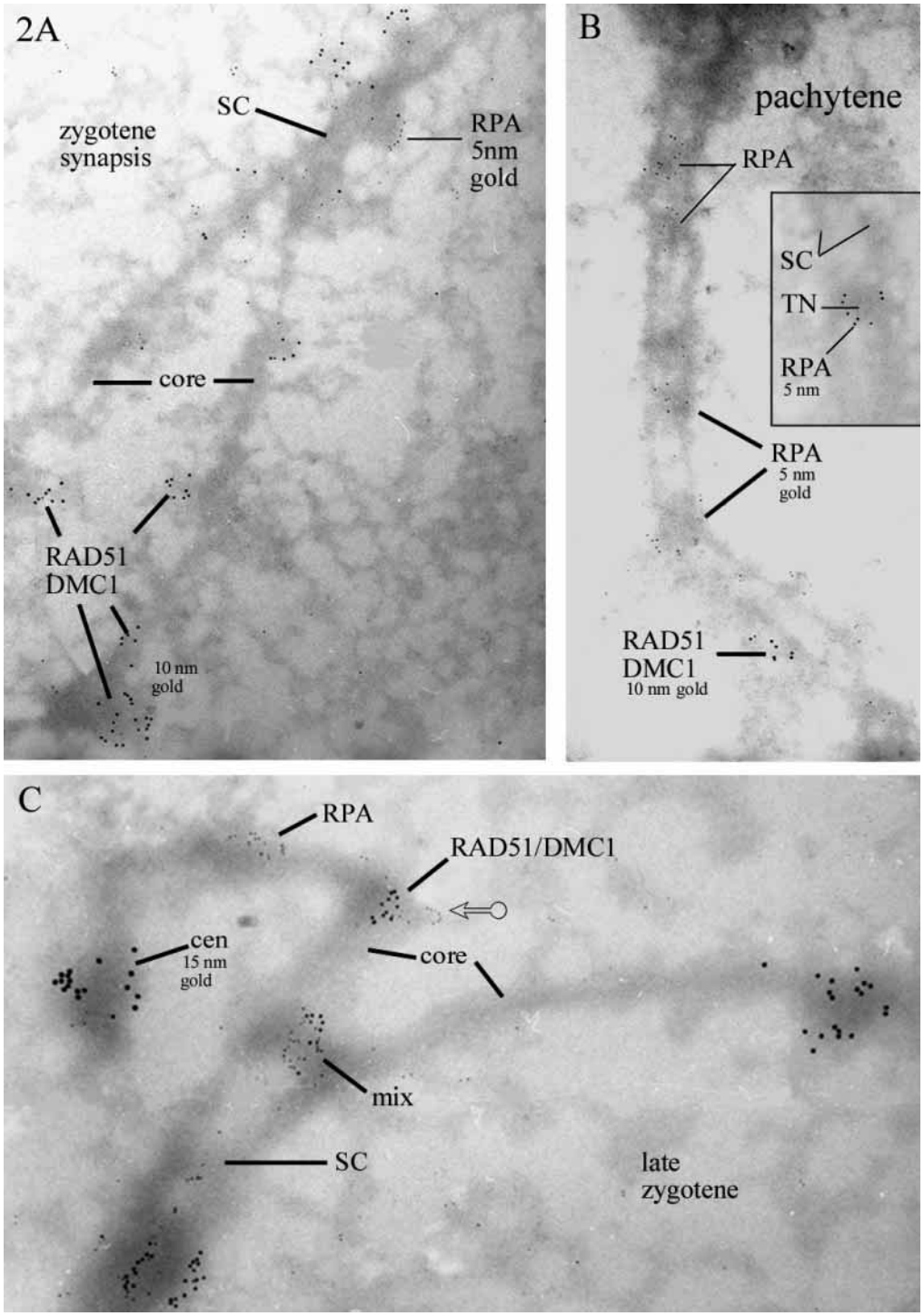

Fig. 2. Immunoelectron microscopy of RAD51/DMC1 (10 nm gold grains) and RPA (5 nm gold grains) in association with chromosome cores/SCs in an early and later meiotic prophase spermatocyte. (A) At early meiotic prophase, there is an abundance of RAD51/DMC1 foci but relatively few RPA foci in association with partially paired zygotene chromosome cores and SCs. (B; insert) At a later stage, pachytene, there are numerous RPA foci and very few RAD51/DMC1 foci. The RPA foci are concentrated on central element-associated nodules, TN. The width of the SC is about 200 nm. (C) At early pachytene, there are occasionally a few unpaired centromeric ends (15 nm gold grains). One of these 'laggards' is shown to have RPA associated with a single, unpaired chromosome core, indicating that RPA is not always associated with RAD51/DMC1 protein. The image further demonstrates the presence of mixed foci containing RAD51/DMC1 and RPA antigen (mix). Incidental is the observation that RPA gold grains occur as a small loop (arrow) in this and other electron micrographs. The width of the SC is about 200 nm.

associated, immunogold grains. The reverse situation exists at a later stage where fully synapsed chromosome cores contain four RPA foci associated with the SC, but there is only one RAD51/DMC1 focus (Fig. 2B, RAD51/DMC1 10 nm immunogold grains, RPA 5 nm). At the onset of the pachytene stage, there are occasionally a few centromeric ends of chromosomes that have not completed synapsis. Such a 'laggard' is shown in Fig. 2C, which demonstrates the combination of RAD51/DMC1 and RPA protein in single nodules, marked as 'mix' in the figure. The arrow marks a small loop of aligned RPA gold grains, which is not uncommon, but the significance is unclear.

RPA at SC-associated transitional or terminal nodules

Where the chromosome cores are fully synapsed (Fig. 2B), the 5 nm gold grains tend to be concentrated on dense nodes of the central element of the SC, suggesting that the RPA protein is present in some form of nodule (Fig. 2B and insert; Fig. 4D-G). These nodes do not have RAD51/DMC1 protein and

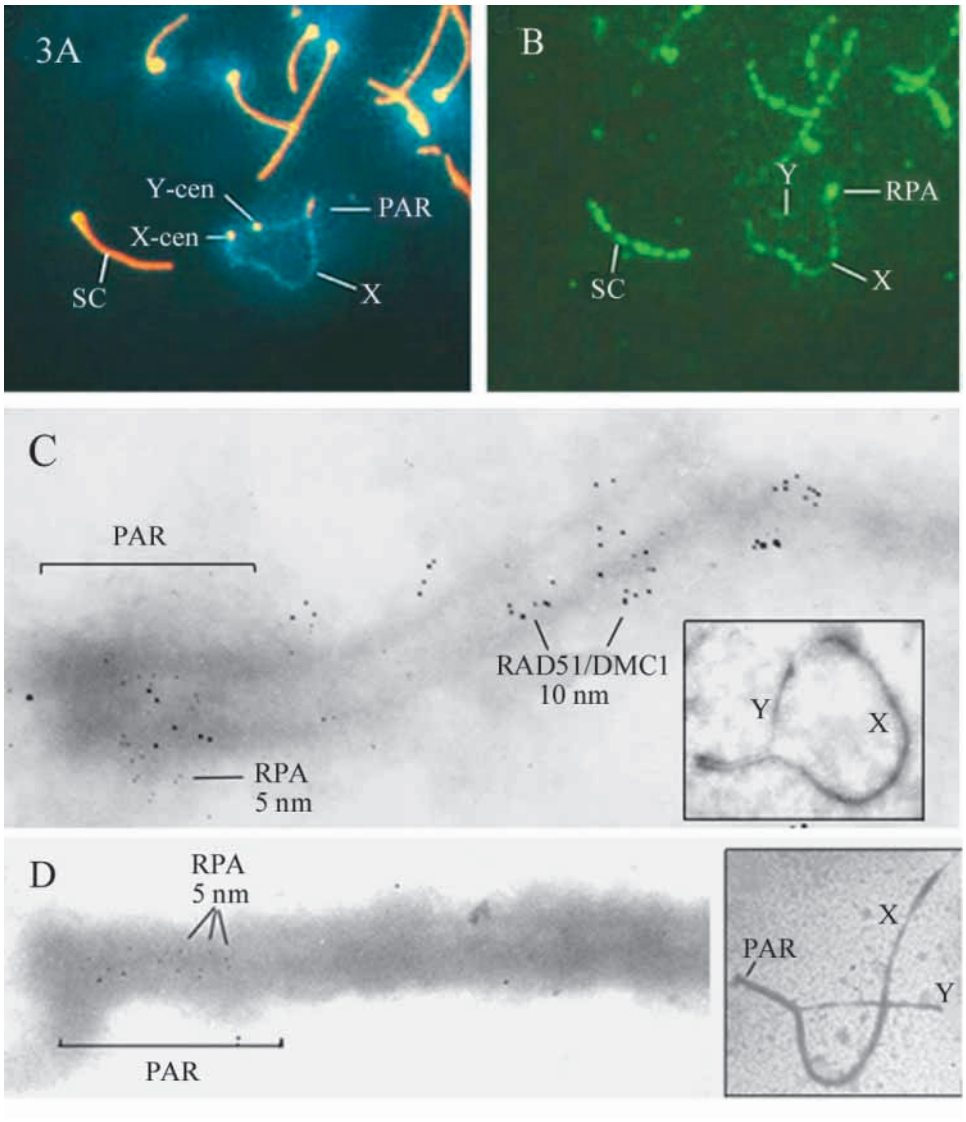

Fig. 3. RPA at the pseudoautosomal region, PAR, of the X-Y chromosomes. (A) Chromosome cores and centromeres visualized with fluorescent tags. The X and Y chromosomes have a short paired region, PAR. (B) The same chromosome visualized with anti-RPA antibody. The autosomal SCs and the unpaired X-chromosome core have numerous RPA foci. The PA region frequently has the brightest RPA focus or foci. Scale: the SCs are about 15 mm in length. (C; insert) At early pachytene there is extensive non-homologous synapsis between the distal portions of the X and Y chromosomes. RPA is present in the most distal portion, presumably the actual PA region. (D; insert) In the rat, the late RNs are better defined than in the mouse, and the Figure illustrates a group of 5 nm RPA gold grains in association with a nodule.

therefore do not conform to the concept of an 'early nodule'. Since they also do not have the MLH1 protein (see below), they therefore do not qualify as 'late nodules'. Few if any of these nodules will persist and they therefore represent some sort of 'terminal' or 'transitional' nodule, TN.

RPA at the X-Y pseudo autosomal region

The short Y chromosome becomes fully synapsed with the distal portion of the long X chromosome during early meiotic prophase, but the two are homologous only at their most distal regions, the pseudo-autosomal (PA) region (Fig. 3). In the laboratory rat and mouse, the PA region has one or more reciprocal recombinant events, which are presumed to regulate the proper segregation of the X and the Y chromosome at the first meiotic division (Soriano et al., 1987). These crossovers are recognized as a chiasma at diplotene and metaphase I. The RPA antigen, marked by green FITC immunofluorescence in Fig. 3B, is clearly present in the terminal segment of the PA region. The immunofluorescence signal is frequently one of the brightest FITC foci of the nucleus, and this may be caused by the presence of two or more proximal foci. Similarly, the PA region has a pronounced BLM signal as reported previously (Moens et al., 2000).

When the X and the Y chromosomes have a long non-homologous pairing segment, there is RAD51/DMC1 antigen (10 nm gold grains) along the length of the paired segment (Fig. 3C) as well as along the core of the X chromosomes. However, RPA is concentrated in the terminal, PA, region (Fig. 3C) and along the X chromosome core (Fig. 3B). In the rat, which has better EM-defined, SC-associated nodules, the RPA can be detected at the nodule in the PA region (Fig. 3D; Fig. 7B).

RPA and BLMp colocalize

Because RPA (this report) and BLMp (Walpita et al., 1999; Moens et al., 2000) are frequently present on the small pseudoautosomal region of the X and Y chromosomes, we tested the possibility that these two proteins regularly occur together in the same protein complex. For this purpose, the BLM antigen was detected by rabbit anti-BLM serum and the secondary antibody was tagged for fluorescent microscopy or for EM observation. The RPA antigen was detected by a mouse serum and differentially tagged secondary antibodies. To assess the relative contribution of each antigen to the individual foci and to be able to quantify the immunogold labeling of foci, we avoid the use of rabbit antibodies against both BLM and RPA protein as in Walpita et al. (Walpita et al., 1999). Superposition of the fluorescent images indicates that most RPA foci also have BLM antigen (Fig. 4). Whereas the RPA signals are generally of similar strength (Fig. 4B), the BLM signals vary widely in intensity (Fig. 4A). For this reason, it is difficult to quantify the contribution of each antigen to the foci by visual evaluation of

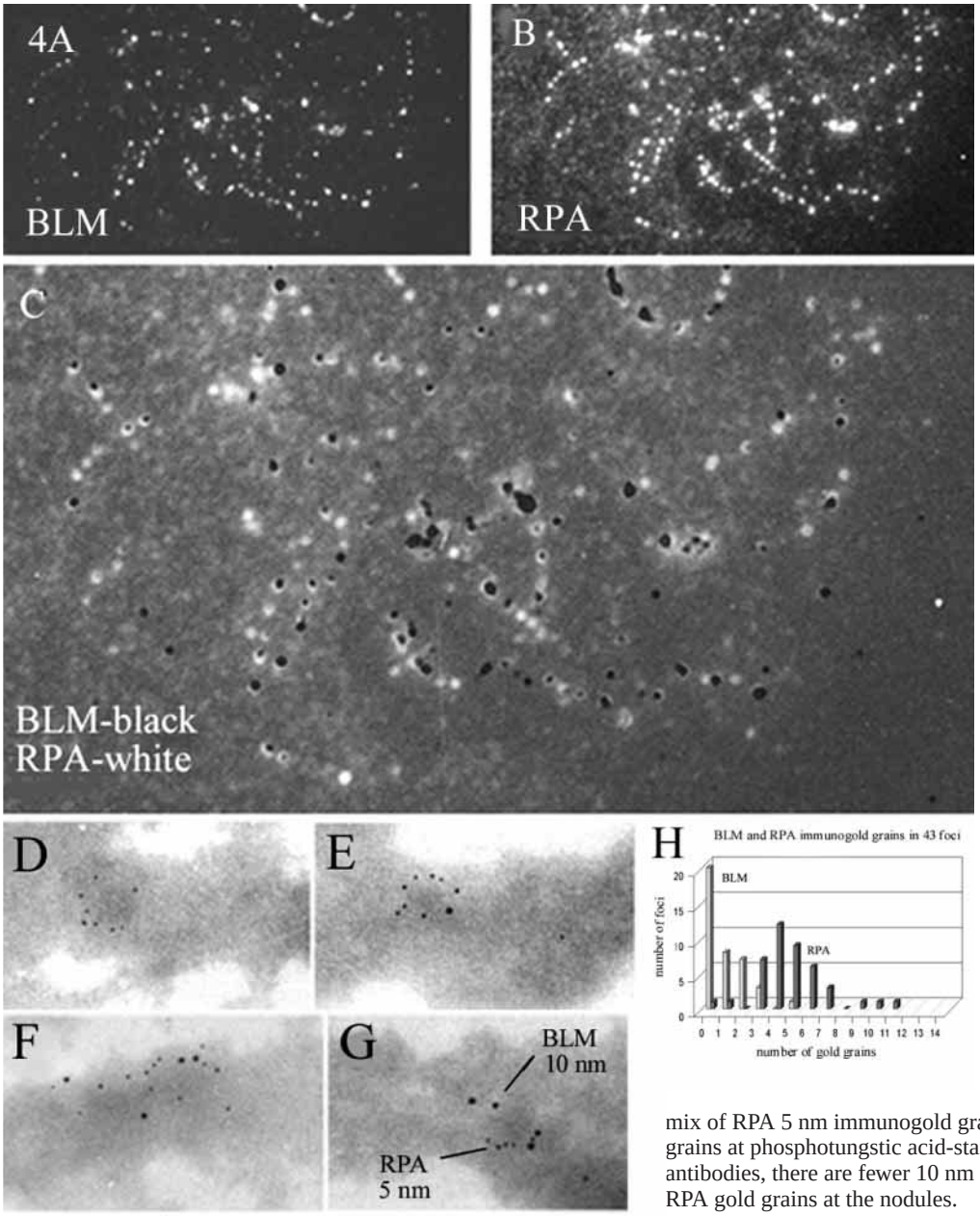

Fig. 4. Colocation of RPA and BLM protein in pachytene spermatocytes. (A,B) The same nucleus immunostained for BLM (A) and for RPA (B). (C) The BLM image of (A) is made into a negative and superimposed on the positive RPA image of (B). Nearly all BLM foci colocate with RPA foci. The relative contributions of the two proteins to the individual foci are semi-quantifiable by the size and the intensity of the immunofluorescent signal, and this is somewhat more efficient than multiple colour combinations. (D-G) Electron micrographs of the mix of RPA 5 nm immunogold grains and 10 nm BLM immunogold grains at phosphotungstic acid-stained SCs and nodules. (H) With our antibodies, there are fewer 10 nm BLM gold grains than there are 5 nm RPA gold grains at the nodules.

subtle colour differences. Instead, we represent the BLM signal intensity by black dots (negative image) and superimpose these dots on the white RPA signals (positive image) (Fig. 4C). This procedure clearly demonstrates that at the level of resolution of immunofluorescence, most BLM foci colocalize precisely with the RPA foci, and there is much variation in the intensity of the BLM signals as indicated by the sizes of the BLM signals.

The colocation of RPA and BLM was confirmed in immunogold-labeled foci, where the two types of gold grains, RPA 5 nm and BLM 10 nm, can be found together in the nodules (Fig. 4E-G). For the antibodies that we use, there are more RPA gold grains per focus than there are BLM gold grains (Fig. 4H).

MSH4 co-locates with RPA in transitional nodules

The meiosis-specific MSH4p homologue of *E. coli* MutSp is required for synapsis and recombination. In mouse it is present along the paired chromosome cores at meiotic prophase (Fig. 5) (Kneitz et al., 2000) (S. Santucci-Darmanin, P.B.M., F. L. Lespinasse et al., unpublished). MSH4 fluorescent foci appear at the time that the early nodules are losing the RAD51/DMC1 component. Biochemical evidence suggests that there is an interaction between the two types of proteins (S. Santucci-Darmanian, P.B.M., F. L. Lespinasse et al., unpublished), but it is relatively rare to find co-location of the two types of proteins either with fluorescent microscopy (Fig. 5C) or with electron microscopy (Fig. 5D,E), when the two antigens are differentially labeled. However, it is evident that MSH4 and RPA frequently co-locate to the same foci when observed with fluorescent microscopy (Fig. 5A) or electron microscopy (Fig. 5B). It is concluded that MSH4 is mostly a component of the transition/terminal nodules. Because the TNs vanish during meiotic prophase, it is possible that MSH4, in concert with

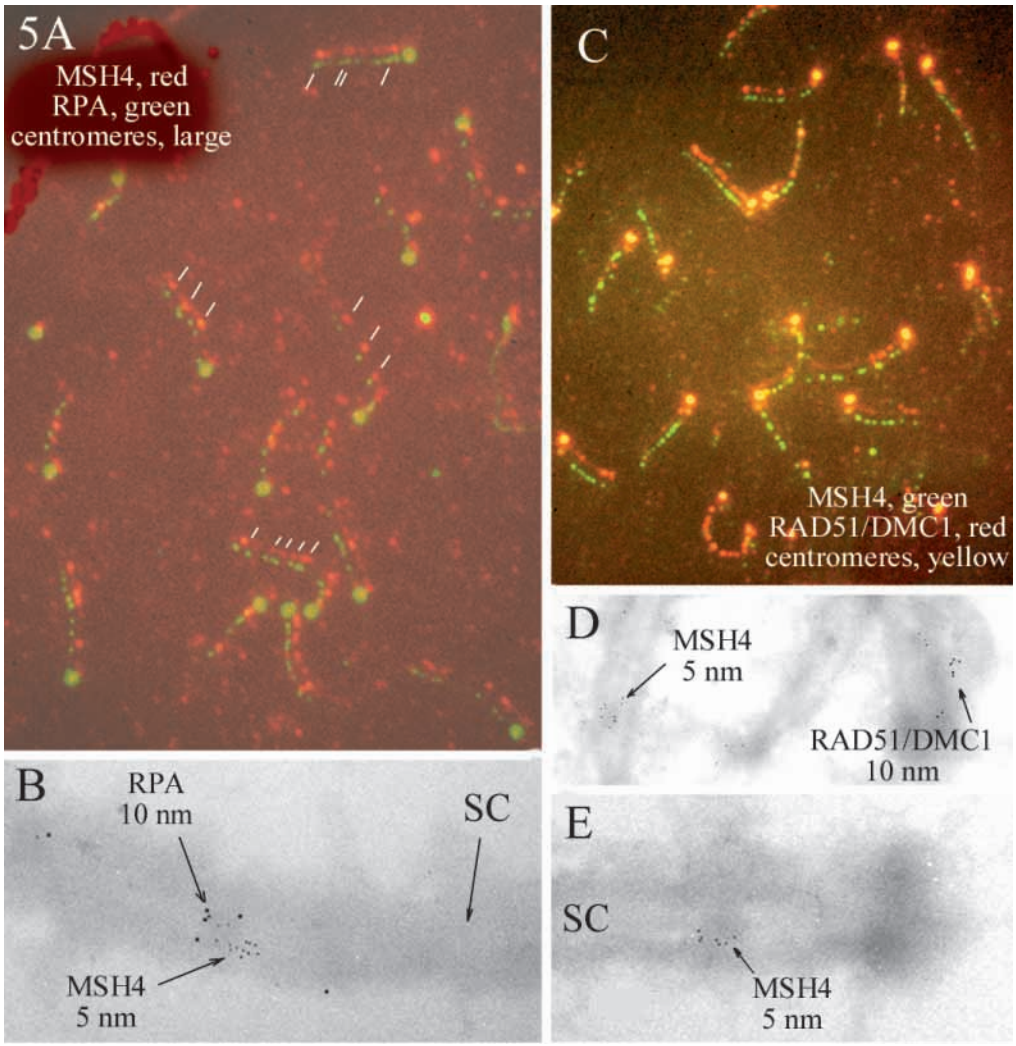

Fig. 5. The association of MSH4p with RPA and RAD51/DMC1p. (A) The images of the red MSH4 foci and the green RPA foci are slightly offset to better demonstrate the colocation of the two types of foci. The short white lines indicate the direction of the offset and examples of colocating foci. The large bright green foci are the centromeres. (B) The colocation is also evident with immune electron microscopy. The 10 nm gold particles mark RPA antigen and the 5 nm grains mark the MSH4 antigen. The grains are associated with a transitional nodule at the central region of the SC. (C) The association of RAD51/DMC1 with MSH4 foci is less pronounced, and evidence from counts of five complete nuclei with some 150 foci each suggest that at most 10% of the foci possibly overlap and that, in general, the MSH4 foci appear after the Rad51/DMC1 foci have declined in numbers. The X chromosome at the base of (C) has, as usual, prolonged presence of RAD51/DMC1 foci. (D,E) At the EM level MSH4 foci (5 nm gold) are mostly separate from RAD51/DMC1 foci (10 nm gold). (E) The MSH4 antigen is associated with the transitional nodule, which has no evidence of RAD51/DMC1 antigen in this double-labeled preparation.

RPA, BLM and others, functions in the resolution of early DNA-DNA interactions.

Time course of RPA and BLM versus MLH1

Immunocytologically detectable MLH1 foci that are in association with the SCs appear in the later part of meiotic prophase after RAD51/DMC1 foci are no longer present, and their numbers, about 23 per nucleus, are small in comparison with the numbers of other foci. In general, it appears that RPA foci are already reduced to small numbers when MLH1 foci first appear (Fig. 1F). The nucleus in Fig. 6A has four RPA foci marked by arrows and 22 MLH1 foci, nearly the full complement. There appears to be no positional correspondence between RPA and MLH1 foci. Electron microscopy, however, shows the occasional presence of RPA in RNs (Fig. 3D; Fig. 7B). The BLM foci persist longer than the RPA foci (Fig. 1F), and they are still present when the MLH1 foci develop (Fig. 6B). From immunofluorescent observations, there is no clear indication that the two types of foci colocate (Fig. 6B). The BLM foci decline in numbers, whereas the MLH1 foci remain fairly constant (Fig. 6D). Although the MLH1 foci normally remain until the onset of the diplotene stage in male meiosis, they persist into the diplotene stage of female meiosis.

MLH1 protein is a component of EM-defined late recombination nodules

EM of late pachytene mouse SCs treated with anti-MLH1 monoclonal antibody and secondary goat anti-mouse antibody tagged with 5 nm gold grains show that the MLH1 antigen is located at the EM-defined late RNs. (Fig. 6C,E-G). The presence of the MLH1 antigen is remarkably predictable. Where one SC of a given nucleus is found to have an MLH1-labeled RN, all other SCs of that nucleus predictably have one or two such RNs. This was confirmed in more than 20 nuclei. The exact localization of an MLH1-labeled RN to the point of a presumptive chiasma is demonstrated in Fig. 6F and G. Normally RNs are no longer present at the diplotene stage in the male, but when the diplotene configurations are induced precociously by the phosphatase inhibitor okadaic acid in purified early prophase cells, the MLH1 foci are still present at diplotene. The platinum/gold shadow casting enhances the appearance of the RNs in the rat (Fig. 7), but the mouse nodules are somewhat smaller and are less well defined with this

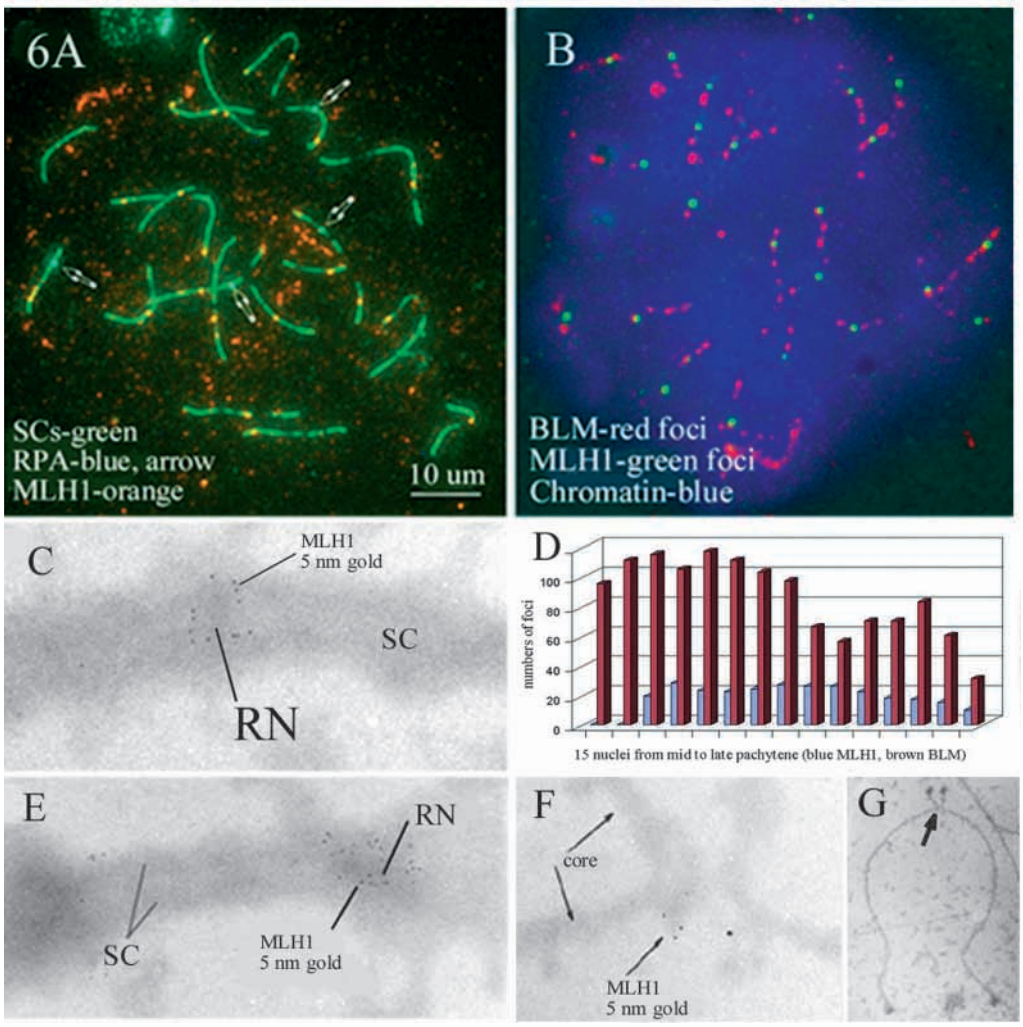

Fig. 6. MLH1, RPA and BLM foci at meiotic prophase. (A) MLH foci (orange) appear in association with the SCs (green) when there are only a very few RPA foci (blue) left and there is no obvious colocation at this time. (B) BLM foci (red) are still fairly abundant when the MLH1 foci (green) are present in their nearly full complement of 20-30 foci. There does not appear to be colocation of BLM with MLH1. (C,E) Evidence that MLH1 antigen, which is marked by 5 nm gold grains, locates to the EM-defined RNs. The RNs are the dark-stained (PTA) bodies in association with the SCs. In the nuclei that are positive for MLH1, each SC has one or two immunogold labeled RNs. (D) The bar graph illustrates the decline in immunofluorescent BLM foci, whereas the numbers of MLH1 foci remain relatively constant at late pachytene. (F,G) A precocious diplotene bivalent that was generated by a 2 hour okadaic acid treatment of a pachytene bivalent demonstrates the presence of an MLH1-labeled RN at the site of a presumptive chiasma/crossover.

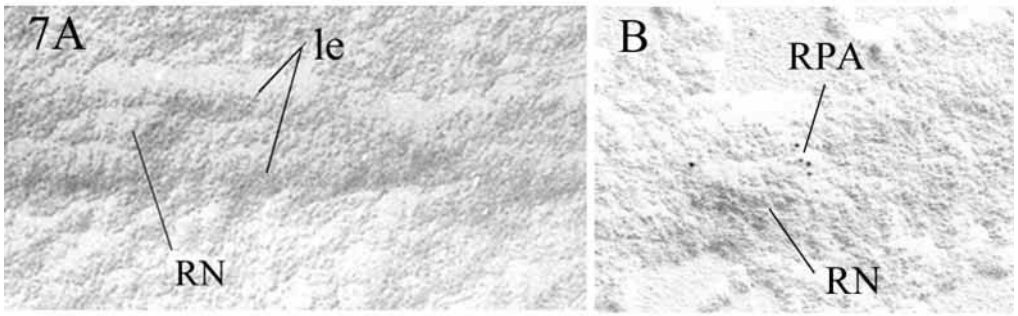

Fig. 7. Definition of a rat recombination nodule, RN, in a shadow-cast preparation of an SC. (A) The SC consists of two lateral elements, le, and a median central element. (B) Occasionally RPA can be detected at these RNs. Mouse RNs are somewhat smaller and less distinct and are therefore visualized with PTA in the other illustrations. The width of the SC is about 200 nm.

methodology. Therefore the alternative, PTA staining, was used to visualize mouse nodules and associated immunogold grains in Figs 2-6.

Discussion

At issue is the question of how the numerous early DNA-DNA interactions at meiotic prophase are resolved so that only a few reciprocal recombination events are present at late prophase. The initiation of early DNA-DNA interactions in yeast and mice has been demonstrated to follow the double-strand break (DSB) model by SPO11 transesterase induction of breaks (Keeney et al., 1997; Mahadevaiah et al., 2001). Following 5′ strand resection, the 3′ single-stranded overhangs are then coated with RAD51 and DMC1 proteins, and these function in homology search and joint molecule formation (Bishop, 1994; Schwacha and Kleckner, 1997). Deletion of SPO11 in mice results in the absence of RAD51/DMC1 foci that are normally

detected at the cores and SCs of the meiotic prophase chromosomes (Baudat et al., 2000). Because homologous chromosome synapsis is disrupted in these mice, it might indicate that the RAD51/DMC1 sites function in synapsis (Baudat et al., 2000; Romanienko and Camerini-Otero, 2000). On the basis of the correlation between SC lengths and numbers of RAD51/DMC1 foci in six plant species with widely divergent genome sizes, Anderson et al. (Anderson et al., 2001) have also suggested that these early interactions function in chromosome synapsis. Subsequently, most or all of the DNA-DNA interactions evidently are resolved without reciprocal recombination.

In the double-strand break model, the joint molecules can be resolved in a number of ways by specific enzymatic complexes. Depending on how the two Holliday junctions of a joint molecule are cleaved, there can be a 1:1 ratio of reciprocal to non-reciprocal recombinants. Taking into account the preferential resolution that causes deviations from the 1:1 ratio, there would still be a large excess of reciprocal recombinations produced by the 250 RAD51/DMC1 sites in the mouse where an average of only about 23 reciprocal events are observed. It has been argued, however, that the joint molecules can also be resolved without reciprocal recombination along different pathways (Gilbertson and Stahl, 1996). These pathways require helicase and topoisomerase functions, and are therefore of particular interest to us because of the observed association of Bloom RecQ helicase with RAD51/DMC1 sites at the cores/SCs of meiotic prophase chromosomes (Moens et al., 2000).

Bloom protein normally functions in chromosome stability by the removal of DNA conformations that could lead to chromosome rearrangements or recombination. BLM protein, as a member of the family of RecQ helicases, belongs to a class of anti-recombinases (Constantinou et al., 2000) that could function to resolve the meiotic prophase chromosome interaction without reciprocal recombination, analogous to the yeast RecQ helicase SGS1 that can resolve strand invasion events (Frei and Gasser, 2000). Mutations of the *BLM* gene lead to chromosome rearrangements and characteristically high levels of sister chromatid exchanges in somatic cells (German, 1993; Watt et al., 1996). BLM RecQ helicase and topoisomerase IIIa interact physically and functionally to enable passage of double-stranded DNA in somatic and meiotic human cells (Harmon et al., 1999; Johnson et al., 2000). Thus the complex demonstrably suppresses recombination and is therefore an appropriate candidate for the resolution of early DNA-DNA interactions at meiotic prophase.

We observe that RAD51/DMC1 foci become associated with RPA and somewhat later with BLMp. This observation can be related to the reports that RecQ helicases interact with RPA. Brosh et al. (Brosh et al., 2000) have shown that in vitro the presence of RPA stimulates the helicase activity of BLMp, and Constantino et al. (Constantino et al., 2000) show that the RecQ helicases WRN and BLM localize to RPA foci, where they promote translocation of the Holliday junctions and dissociate recombination intermediates. Similarly, Sakamoto et al. (Sakamoto et al., 2001) report that WRNp colocalizes with RPA foci at sites of induced DNA damage. Taken together, these observations provide support for the hypothesis that early meiotic prophase DNA-DNA interactions are resolved, without reciprocal recombination, by a protein complex that includes RPA and BLMp, which probably acts in conjunction with topoisomerase IIIa.

Although it is well established that MSH4p is a partner of the RPA/BLM complex and the TNs (Fig. 5C,D,E), its function in the complex is uncertain (S. Santucci-Darmanin, P.B.M., F. L. Lespinasse et al., unpublished). At later stages when few MSH4 foci remain, it has been reported that they colocalize with MLH1p but here, too, the functions are still speculative (Santucci-Darmanin, 2000).

Origin of recombination nodules

Because MLH1 protein is associated with recombinant events and because the MLH1 foci are correlated in number and distribution with reciprocal recombinant events, it has been hypothesized that the MLH1 foci represent the RNs in mice (Anderson et al., 1999). We provide evidence in support of that hypothesis by showing that the MLH1 antigen is present in EM-defined RNs (Fig. 6C,E) and that the RN and the MLH1 protein are present at the site of a chiasma (Fig. 6F,G). In $MLH1^{-/-}$ mice, chromosome synapsis is normal. The repulsion of homologues at the onset of meiosis appears normal but subsequently there is a complete or near complete lack of chiasmata, and the result is an accumulation of univalents in the nucleus (Baker, 1996; Edelmann et al., 1996). Apparently, reciprocal recombinant events are mostly absent.

It is evident that most early DNA-DNA interactions that are recognized as RAD51/DMC1 foci are resolved by mid prophase. At a later stage, the foci that correspond to RNs are observed. The question arises whether (1) a subset of the early interactions persist and become late RNs or (2) whether the late RNs arise de novo. There is support for both propositions.

(1) The EM data on RAD51/DMC1 and RPA immunogold grains in Fig. 1E and Fig. 2 suggest that the early RAD51/DMC1 nodules acquire RPA, and eventually no RAD51/DMC1 component is present in the nodules. These nodules also acquire BLM and MSH4 protein, and we interpret from this that the function of these transitional nodules is the removal of early DNA-DNA interactions without reciprocal recombination (see above). There does not seem to be a distinct colocation of the RPA-BLM foci with the MLH1 foci as demonstrated in Fig. 6A and B. This would suggest that interactions that are being resolved do not become late RNs. A second round of SPO11-RAD51/DMC1 function would be required to initiate new DSBs. There is no clear evidence for this other than the presence of SPO11 on SCs at mid pachytene (Romanienko and Camerini-Otero, 2000).

(2) Although the RPA and BLM proteins do not show a continuous presence into the RNs, the MSH4 component has been reported to colocalize with MLH1 (Santucci-Darmanin et al., 2000). This would argue for the progression of a select few TNs into RNs. We also observe the presence of RPA in some RNs (Fig. 3D; Fig. 7B), but we cannot determine if this represents continuity or newly acquired RPA in the standard context of DNA metabolic activity.

These observations on the origins of RNs are clearly related to but do not yet resolve the issue of genetic and crossover interference. They suggest that in the appropriate organisms or experimental conditions, the immunocytology of recombination-related proteins could elucidate the mechanisms of interference that limit and position the crossovers.

We gratefully acknowledge the contributions of antibodies for this study: anti-BLM by Raimundo Freire (Facultad de Medicina, Tenerife), rabbit anti-hRPA by Jim Ingles (Banting and Best Institute, Toronto) and rabbit anti-hMNH4 by Veronique Paquis (UMR CNRS, Nice). The shadow-casting of SCs was performed by York undergraduate student, Mike Sebastian, and York EM technical assistant, Karen Rethoret. The research was funded by NSERC of Canada.

References

Albini, S. M. and Jones, G. H. (1988). Synaptonemal complex spreading in *Allium cepa* and *A. fistulosum*. II. Pachytene observations: The SC karyotype and the correspondence of late recombination nodules and chiasma. *Genome* **30**, 399-410.

Anderson, L. K., Offenberg, H. H., Verkuijlen, W. M. H. C. and Heyting, C. (1997). RecA-like proteins are components of early meiotic nodules in lily. *Proc. Natl. Acad. Sci. USA* **94**, 6868-6873.

Anderson, L. K., Reeves, A., Webb, L. M. and Ashley, T. (1999). Distribution of crossing over on mouse synaptonemal complexes using immunofluorescent localization of MLH1 protein. *Genetics* **151**, 1569-1579.

Anderson, L. K., Hooker, K. D. and Stack, S. M. (2001). The distribution of early recombination nodules on zygotene bivalents from plants. *Genetics* **159**, 1259-1269.

Ashley, T., Plug, A. W., Xu, J., Solari, A. J., Redy, G., Golub, E. I. and Ward, D. C. (1995). Dynamic changes in Rad51 distribution on chromatin during meiosis in male and female vertebrates. *Chromosoma* **104**, 19-28.

Baker, S. M., Bronner, C. E., Zhang, L., Plug, A. W., Robatzek, M., Warren, G., Elliott, E. A., Yu, J., Ashley, T., Arnheim, N., Flavell, R. A. and Liskay, R. M. (1995). Male mice defective in the DNA mismatch repair gene PMS2 exhibit abnormal chromosome synapsis in meiosis. *Cell* **82**, 309-319.

Barlow, A. L., Benson, F. E., West, S. C. and Hulten, M. A. (1997). Distribution of the Rad51 recombinase in human and mouse spermatocytes. *EMBO J.* **16**, 5207-5215.

Baudat, F., Manova, K., Yuen, J. P., Jasmin, M. and Keeney, S. (2000). Chromosome synapsis defects and sexually dimorphic meiotic progression in mice lacking spo11. *Mol. Cell* **6**, 989-998.

Bishop, D. K. (1994). RecA homologs Dmc1 and Rad51 interact to form multiple nuclear complexes prior to meiotic chromosome synapsis. *Cell* **79**, 1081-1092.

Brosh, R. M., Jr, Li, J. L., Kenny, M. K., Karow, J. K., Cooper, M. P., Kureekattil, R. P., Hickson, I. D. and Bohr, V. A. (2000). Replication protein A physically interacts with Bloom's syndrome protein and stimulates its helicase activity. *J. Biol. Chem.* **275**, 23500-23508.

Carpenter, A. T. C. (1975). Electron microscopy of meiosis in *Drosophila melanogaster* females II. The recombination nodule – a recombination-associated structure at pachytene? *Proc. Natl. Acad. Sci. USA* **72**, 3186-3189.

Carpenter, A. T. C. (1979). Recombination nodules and synaptonemal complex in recombination-defective females of *Drosophila melanogaster*. *Chromosoma* **75**, 259-292.

Clermont, Y. (1972). Kinetics of spermatogenesis in mammals: Seminiferous epithelium cycle and spermatogonial renewal. *Physiol. Rev.* **52**, 198-236.

Constantinou, A., Tarsounas, M., Karow, J. K., Brosh, R. M., Bohr, V. A., Hickson, I. D. and West, S. C. (2000). Werner's syndrome protein (WRN) migrates Holliday junctions and co-localizes with RPA upon replication arrest. *EMBO reports* **1**, 1-5.

Counce, S. and Meyer, G. F. (1973). Differentiation of the synaptonemal complex and the kinetochore in *Locusta* spermatocytes studied by whole mount electron microscopy. *Chromosoma* **44**, 231-253.

Dobson J. M., Pearlman, R. E., Karaiskakis, A., Spyropoulos, B. and Moens, P. B. (1994). Synaptonemal complex proteins: occurrence, epitope mapping and chromosome disjunction. *J. Cell Sci.* **107**, 2749-2760.

Dresser, M. E. and Moses, M. J. (1980). Synaptonemal complex karyotyping in spermatocytes of the Chinese hamster (*Cricetulus griseus*). IV. Light and electron microscopy of synapsis and nucleolar development by silver staining. *Chromosoma* **76**, 1-22.

Edelmann, W., Cohen, P. E., Kane, M., Lau, K., Morrow, B., Bennett, S., Umar, A., Kunkel, T., Cattoretti, G., Changanti, R. et al. (1996). Meiotic pachytene arrest in MLH1-deficient mice. *Cell* **85**, 1125-1134.

Frei, C. and Gasser, S. M. (2000). RecQ helicases: the DNA replication checkpoint connection. *J. Cell Sci.* **113**, 2641-2646.

German, J. (1993). Bloom syndrome, a Mendelian prototype of somatic mutational disease. *Medicine* **71**, 393-406.

Gilbertson, L. A. and Stahl, F. W. (1996). A test of the double-strand break repair model for meiotic recombination in *Saccharomyces cerevisiae*. *Genetics* **144**, 27-41.

Haaf, T., Golub, E. I., Reddy, R. G., Radding, G. M. and Ward, D. C. (1995). Nuclear foci of mammalian Rad51 recombination protein in somatic cells after DNA damage and its localization in synaptonemal complexes. *Proc. Natl. Acad. Sci. USA* **92**, 2298-2302.

Harmon, F. G., DiGate, R. J. and Kowalczykowsky, S. C. (1999). RecQ helicase and topoisomerase III compromise a novel DNA strand passage function: a conserved mechanism for control of DNA recombination. *Mol. Cell* **3**, 611-620.

He, F. G., Henricksen, L. A., Wold, M. S. and Ingles, C. J. (1995). RPA involvement in the damage-recognition and incision steps of nucleotide excision repair. *Nature* **374**, 566-569.

Heyting, C., Dietrich, A. J. J., Moens, P. B., Dettmers, R. J., Offenberg, H. H., Redeker, E. J. W. and Vink, A. C. G. (1988). Synaptonemal complex proteins. *Genome* **31**, 81-87.

Henricksen, L. A., Umbricht, C. B. and Wold, M. S. (1994). Recombinant replication protein A: expression, complex formation, and functional characterization. *J. Biol. Chem.* **269**, 11121-11132.

Johnson, F. B., Lombard, D. B., Neff, N. F., Mastrangelo, M.-A., Dewolf, W., Ellis, N. A., Marciniak, R. A., Yin, Y., Jaenisch, R. and Guarente, L. (2000). Association of the Bloom Syndrome protein with topoisomerase IIIa in somatic and meiotic cells. *Cancer Res.* **60**, 1162-1167.

Jones, G. H. (1987). Chiasmata. In Meiosis (ed. P. B. Moens), pp. 213-238. Orlando, USA: Acad. Press. Inc.

Keeney, S., Giroux, C. N. and Kleckner, N. (1997). Meiosis-specific DNA double-strand breaks are catalyzed by Spo11, a member of a widely conserved protein family. *Cell* **88**, 375-384.

Kovalenko, O. V., Plug, A. W., Haaf, T., Gonda, D. K., Ashley, T., Ward, D. C., Radding, C. M. and Golub, E. I. (1996). Mammalian ubiquitin-conjugating enzyme Ubc9 interacts with Rad recombination protein and localizes in synaptonemal complexes. *Proc. Natl Acad. Sci. USA* **93**, 2958-2963.

Kneitz, B., Cohen, P. E., Avdievich, E., Liyin, Z., Kane, M. F., Hou, H., Jr, Kolodner, R. D., Kucherlapati, R., Pollard, J. W. and Edelmann, W. (2000). MutS homolog 4 localization to meiotic chromosomes is required for chromosome pairing during meiosis in male and female mice. *Genes Dev.* **14**, 1085-1097.

Kremer, E. J. and Kistler, W. S. (1991). Localization of mRNA for testis specific histone H1t by in situ hybridization. *Exp. Cell Res.* **197**, 330-332.

Mahadevaiah, S. K., Turner, J. M., Baudat, F., Rogakou, E. P., de Boer, P., Blanco-Rodriguez, J., Jasin, M., Keeney, S., Bonner, W. M. and Burgoyne, P. S. (2001). Recombinational DNA double-strand breaks in mice precede synapsis. *Nat. Genet.* **27**, 271-276.

Moens, P. B. (1978). Lateral element cross connections of the synaptonemal complex and their relationship to chiasmata in rat spermatocytes. *Can. J. Genet. Cytol.* **20**, 567-579.

Moens, P. B. (1995). Histones H1 and H4 of surface spread chromosomes. *Chromosoma* **104**, 169-174.

Moens, P. B., Heyting, C., Dietrich, A. J. J., van Raamsdonk, W. and Chen, Q. (1987). Synaptonemal complex antigen location and conservation. *J. Cell Biol.* **105**, 93-103.

Moens, P. B., Chen, D. J., Shen, Z., Kolas, N., Tarsounas, M., Heng, H. H. Q. and Spyropoulos, B. (1997). RAD51 immunocytology in rat and mouse spermatocytes and oocytes. *Chromosoma* **106**, 207-215.

Moens, P. B., Freire, R., Tarsounas, M., Spyropoulos, B. and Jackson, S. P. (2000). Expression and nuclear localization of BLM, a chromosome stability protein mutated in Bloom's syndrome, suggest a role in recombination during meiotic prophase. *J. Cell Sci.* **113**, 663-672.

Pittman, D. L., Cobb, J., Schimenti, K. J., Wilson, L. A., Cooper, D. M., Brignull, E., Handel, M. A. and Schimenti, J. C. (1998). Meiotic prophase arrest with failure of chromosome synapsis in mice deficient for DMC1, a germline-specific RecA homolog. *Mol. Cell* **5**, 697-705.

Plug, A. W., Peters, A. H. F. M., Yang, X., Keegan, K. S., Hoekstra, M. F., Baltimore, D., de Boer, P. and Ashley, T. (1997). ATM and RPA in meiotic chromosome synapsis and recombination. *Nat. Genet.* **17**, 457-461.

Plug, A. W., Peters, A. H. F. M., Keegan, K. S., Hoekstra, M. F., de Boer, P. and Ashley, T. (1998). Changes in the protein composition of meiotic nodules during mammalian meiosis. *J. Cell Sci.* **111**, 413-423.

Romanienko, P. J. and Camerini-Otero, R. D. (2000). The mouse SPO11 gene is required for meiotic chromosome synapsis. *Mol. Cell* **6**, 975-987.

Sakamoto, S., Nishikawa, K., Heo, S. J., Goto, M., Furuichi, Y. and

Shimamoto, A. (2001). Werner helicase relocates into nuclear foci in response to DNA damaging agents and co-localizes with RPA and RAD51. *Genes Cells* **6**, 421-430.

Santucci-Darmanin, S., Walpita, D., Lespinasse, F., Desnuelle, C., Ashley, T. and Paquis-Flucklinger, V. (2000). MSH4 acts in conjunction with MLH1 during mammalian meiosis. *FASEB J.* **14**, 1539-1547.

Soriano, P., Keitges, E. A., Schorderet, D. F., Harbers, K., Gartler, S. M. and Jaenisch, R. (1987). High rate of recombination and double crossovers in the mouse pseudoautosomal region during male meiosis. *Proc. Natl. Acad. Sci. USA* **84**, 7218-7220.

Schwacha, A. and Kleckner, N. (1997). Interhomolog bias during meiotic recombination: meiotic functions promote a highly differentiated interhomolog-only pathway. *Cell* **90**, 1123-1135.

Tarsounas, M., Pearlman, R. E., Gasser, P. J., Park, M. S. and Moens, P. B. (1997). Protein-protein interactions in the synaptonemal complex. *Mol. Biol. Cell* **8**, 1405-1414.

Tarsounas, M., Morita, T., Pearlman, R. E. and Moens, P. B. (1999a). Rad51 and DMC1 form mixed complexes associated with mouse meiotic chromosome cores and synaptonemal complexes. *J. Cell Biol.* **147**, 207-219.

Tarsounas, M., Pearlman, R. E. and Moens, P. B. (1999b). Meiotic activation of rat pachytene spermatocytes with okadaic acid: the behaviour of synaptonemal complex components SYN1/SCP1 and COR1/SCP3. *J. Cell Sci.* **112**, 423-434.

Turner, J. M., Mahadevaiah, S. K., Benavente, R., Offenberg, H. H., Heyting, C. and Burgoyne, P. S. (2000). Analysis of male meiotic 'sex body' proteins during XY female meiosis provide insights into their functions. *Chromosoma* **109**, 426-432.

Walpita, D., Plug, A. W., Neff, N. F., German, J. and Ashley, T. (1999). Bloom's syndrome protein, BLM, colocalizes with replication protein A in meiotic prophase nuclei of mammalian spermatocytes. *Proc. Nat. Acad. Sci. USA* **96**, 5622-5627.

Watt, P. M., Hickson, I. D., Borts, R. H. and Louis, E. J. (1996). SGS1, a homolog of the Bloom's and Werner's Syndrome genes, is required for maintenance of genome stability in *Saccharomyces cerevisiae*. *Genetics* **144**, 935-945.